Proc. Natl. Acad. Sci. USA
Vol. 91, pp. 1549–1553, February 1994
Biophysics

Stiffness changes of the cupula associated with the mechanics of hair cells in the fish lateral line

(nonlinear cupular motion/laser interferometry/mechanoreception/gating spring)

SIETSE M. VAN NETTEN[†‡] AND SHYAM M. KHANNA[§]

[†]Department of Biophysics, University of Groningen, The Netherlands; and [§]College of Physicians and Surgeons, Columbia University, New York, NY 10032

Communicated by A. J. Hudspeth, November 16, 1993 (received for review October 9, 1992)

ABSTRACT **Cupular vibration in the lateral-line canal of fish was measured in response to motion of the fluid in the canal by laser-heterodyne interferometry. The results show that the mechanical output/input ratio of the cupula depends on the stimulus amplitude; the cupula thus behaves nonlinearly. The nonlinearity is due to the hair bundles, since it disappears when the cupula is uncoupled from the underlying hair cells. A model of cupular dynamics in which the behavior of the gating springs of the hair cells is incorporated predicts nonlinear responses that are similar to the measurements, suggesting that the nonlinear behavior of the cupula may be attributed to the opening and closing of the transduction channels of the hair cells.**

Vertebrates utilize sensory organs with hair cells to detect a variety of mechanical stimuli from their environment. Examples of these are the auditory, vestibular, and lateral-line systems. The characteristic organelles of hair cells are the stereocilia, pivoting around their insertion points in the cuticular plate that forms the apical end of the cell. Deflection of the stereocilia opens and closes the mechanoelectrical transduction channels (for reviews see refs. 1–3).

The channels responsible for gating the transduction current are located somewhere near the tips of the hair bundles (4, 5) and are possibly associated with the mechanical links connecting the tips of the individual stereocilia in a hair bundle (6). Deflection of the hair bundle would produce mechanical stress in these tip links and could therefore open a transduction channel attached to it.

Corey and Hudspeth (7) proposed a two-state model of the kinetics of transduction channels in frog saccular hair cells, in which it is assumed that the free energy difference between the two states varies linearly with the deflection of the hair bundle, so that deflection in the hair bundle's depolarizing direction increasingly favors the population of open states. An elastic element governed by Hooke's law exhibits the required free energy relationship with displacement. Howard and Hudspeth (8) considered the mechanics of such elastic elements (gating springs) positioned between the stereocilia, like the tip links, and predicted a hair bundle stiffness that varies with hair bundle deflection, having a minimum at a bundle position at which half of the transduction channels are open. This predicted nonlinearity in stiffness was confirmed by measurements on isolated frog saccular hair cells (8). Comparable nonlinearities in stiffness of hair cell bundles were observed in cochlear cultures (9).

In the lateral-line canals of fish, the bundles of the sensory hair cells are attached to the base of a cupula, a dome-shaped structure. Water motion around the animal is coupled to the canal fluid, which displaces the cupula, thus producing hair bundle deflection. The dynamics of the cupula has been investigated *in vivo* by laser-heterodyne interferometry (10, 11), and it was found that the displacement of the cupula in response to canal fluid motion can be changed by manipulating the mechanical properties of the hair bundles (12). This result indicated that hair cell micromechanics, combined with the hydrodynamics of the organ, controls the macromechanical response of the cupula. Since the relative distribution of open and closed transduction channels of a hair cell determines the stiffness of its bundle (8, 13), it may be expected that the kinetics of the transduction channels is reflected in the nonlinearity of cupular responses. The lateral-line organ thus provides an opportunity to investigate mechanical properties of the transduction channels *in vivo*.

The present paper describes measurements on the motion of the cupula with a special focus on nonlinearities. To study the nonlinear relationship between the fluid motion and the vibratory response of the cupula, the frequency of the fluid motion can be maintained constant while the amplitude is increased in steps. For a detailed study, the number of steps required will be large. The same information can be obtained by slowly varying the input amplitude over the whole dynamic range of interest. This can be done with an amplitude-modulated wave with a low modulation frequency. The changes in level are continuous and changes in the response can be measured within a short time (one modulation cycle). An output/input relationship can then be derived by taking the ratio of the envelope of the response to that of the stimulus.

To test whether the nonlinear stiffness of the gating springs can account for the experimentally observed nonlinearities, a model of cupular mechanics including the kinetics of the gating springs (14) is used.

MATERIALS AND METHODS

Preparation. To investigate the dynamics of the cupula in the supraorbital lateral-line canal, seven African knife-fish (*Xenomystus nigri*) 10–12 cm long were used. Fish were anesthetized by intraperitoneal injection (24 mg per kg of body weight) of Saffan (Pitman-Moore, Washington Crossing, NJ; cf. ref. 15), maintained in a small tank mounted on a vibration isolated table inside a soundproof room, and respirated artificially. During the experiments, fish were held in place by head and body clamps. The position and orientation of the fish could be adjusted with a two-axis goniometer and an *x*, *y*, *z* micropositioning system (16). The tank was filled with a modified fish Ringer's solution containing 169.0 mM NaCl, 5.0 mM KCl, 3.0 mM $CaCl_2$, 1.5 mM $MgCl_2$, and 10.0 mM Hepes buffer.

Mechanical Stimulation. The canal organ was exposed by partly removing the overlying skin (Fig. 1). Displacements of fluid, which were sinusoidally modulated in amplitude, were

---

The publication costs of this article were defrayed in part by page charge payment. This article must therefore be hereby marked "*advertisement*" in accordance with 18 U.S.C. §1734 solely to indicate this fact.

[‡]To whom reprint requests should be addressed at: Department of Biophysics, Nijenborgh 4, 9747 AG Groningen, The Netherlands.

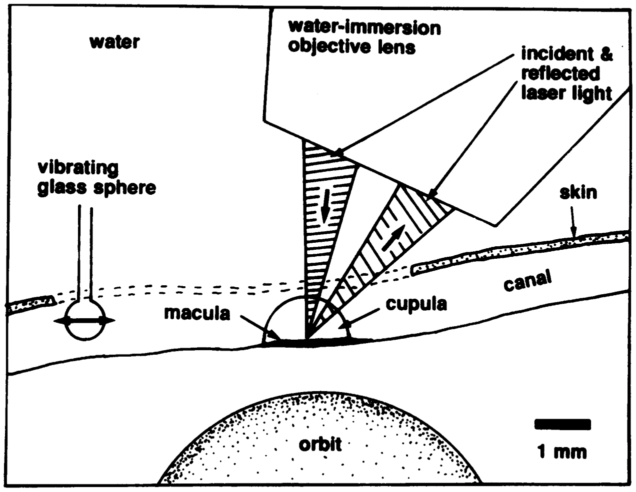

FIG. 1. Scheme for stimulus application and measurement of vibrational responses of the cupula in the supraorbital canal of a living fish underwater. To stimulate the cupula, a glass sphere produces fluid vibrations along the length of the canal. The incident laser beam of a velocity-measuring interferometer is focused on the cupula through one half of the aperture of a water-immersion objective lens, while reflected light is collected by the other half. The direction of visualization and vibration measurement is inclined at an angle of about 70° with respect to the plane of the macula. The region of measurement in the cupula is close to the hair cell bundles.

produced along the longitudinal axis of the canal by a piezoelectrically driven glass sphere ($\phi = 0.8$ mm) located in the canal at a distance of ≈4 mm from the cupula (Fig. 1). Electrical signals to drive the vibrator were synthesized by using a 16-bit D-A converter (Ariel; DSP-16). Carrier frequencies ranged from 30 to 450 Hz, while the modulation frequency (2.4 Hz) and the depth of modulation (100%) were kept constant. Maximum glass-sphere displacement amplitudes were ≈15 μm.

To ascertain that the stimulus generation system is linear, the displacements of the stimulus sphere and of the fluid in the canal were measured. Both responses were found to have a linear relationship with the input voltage.

Vibration Measurements. The sensory epithelium was observed through the transparent cupula in the canal with a slit confocal microscope using reflected light (17, 18). The velocity of the cupula was measured with a laser-heterodyne interferometer (19, 20). The microscope and the interferometer, adjusted so that they are confocal, share a ×20 objective lens (Olympus, New Hyde Park, NY), which is adapted for water immersion with a dipping cone (effective n.a., 0.56). The spot size of the measuring laser beam is ≈2 μm in diameter and the sectioning depth is ≈4 μm. Focusing the microscope a few tens of micrometers above the sensory epithelium in the cupula reveals small, highly reflective regions (21), which were used for vibration measurements because of their closeness to the tips of the hair bundles.

The interferometer measures the velocity of the cupula vibration along the direction of the optical axis of the microscope (Fig. 1). The instrument contains two light beams derived from a mode-stabilized helium/neon laser shifted in frequency with acoustooptic modulators so that their (optical) difference frequency is 1 MHz. The object beam is focused on the moving object. The reflected light is collected by the objective lens, collimated by a pinhole lens arrangement, and interferes with the reference beam at the photodetector, thus producing a 1-MHz signal. When the object is vibrating, the path length of the object beam changes with time and the photodetector signal at 1 MHz is modulated in phase. This signal is applied to a frequency demodulator, thus recovering the instantaneous velocity of the object. Velocity signals were sampled at intervals of 200 μs with a 16-bit A-D converter (Ariel; DSP-16). The equivalent noise level of the interferometer during these experiments was ≈3 $\mu\text{m}\cdot\text{s}^{-1}\cdot\text{Hz}^{-1/2}$.

Fluid displacement was determined by interferometrically measuring the motion of the tip of a very compliant glass probe that closely follows the fluid flow.

Calculation of the Output/Input Ratio of the Cupula. Measured velocity time waveforms are integrated to obtain the cupular displacement. The displacement is high-pass filtered by using a moving average technique to remove components at low frequencies. The envelope of the filtered displacement was recovered by calculating the instantaneous amplitude of the waveform at 4096 points. Squared bin values of the waveform are summed within a time window with a length equal to half the period of the carrier frequency and the sum is divided by the number of bins in this time window. The square root of twice this number is taken as the instantaneous value of the envelope (= $\sqrt{2} \times$ rms amplitude). This value is assigned to a bin at the center of the window. To obtain the value at the other points the window is shifted by one bin at a time and the procedure is repeated, producing the complete envelope of the response. To calculate the envelope at the points at the very beginning and end, the end of the response waveform is folded and connected to the beginning.

The envelope of the cupular response, divided by the envelope of the normalized stimulus ($\sin 2\pi \cdot 2.4 \cdot t$), yields the ratio curve of the output to the input. The ratio curve therefore represents the vibrational amplitude of the cupula, normalized with respect to the maximum amplitude of the amplitude-modulated stimulus.

The shape of the ratio curve immediately reveals whether or not the cupula responds linearly. If the response is linear, the output/input ratio remains constant over a modulation cycle; thus, the ratio curve will be flat. If the cupula responds nonlinearly, the ratio may decrease or increase during a modulation cycle. The ratio at the beginning and end of each modulation cycle is not reliable since the value of the denominator (stimulus envelope) is close to zero.

Furthermore, in the case of a linearly responding cupula, the value of the (flat) ratio curve depends on the carrier frequency. This frequency selectivity is due to the mass-spring system formed by cupular mass and hair bundle stiffness (cf. ref. 22); the ratio increases with (carrier) frequency reaching a maximum at resonance and approaches a constant ratio at higher frequencies.

In the case of a nonlinearly responding cupula, the ratio will be determined by both this frequency selectivity and the nonlinearity.

RESULTS

Output/Input Ratio. The steps taken in the derivation of a ratio curve are shown in Fig. 2. The time axis (0–0.82 s) represents two cycles of modulation. The displacement of the cupula in response to an amplitude-modulated carrier at 107 Hz (Fig. 2*a*) is shown in Fig. 2*b*. The waveforms obtained after high-pass filtering and detection of the envelope are depicted in Fig. 2 *c* and *d*, respectively. The ratio of the envelope of the filtered response to the envelope of the normalized stimulus is shown in Fig. 2*e*. The ratio, as a function of time, is essentially flat except for the large peaks (partly erased) at the beginning and end of a modulating cycle. The flatness of the output/input ratio shows that at this carrier frequency the cupular displacement is linearly related to the applied stimulus.

Nonlinear Responses. Cupular dynamics was studied by using amplitude-modulated fluid flow at different carrier frequencies. The slowly (2.4 Hz) varying envelope of the

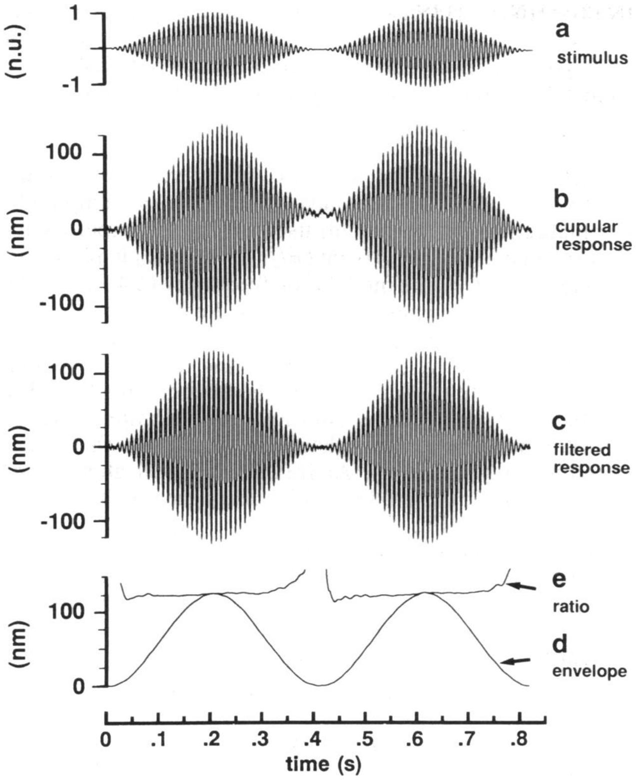

FIG. 2. Time waveforms of stimulus and response at a carrier frequency of 107 Hz and a modulation frequency of 2.4 Hz, of which two cycles are shown. (*a*) Amplitude-modulated stimulus applied to the piezoelectric driver (normalized units). (*b*) Cupular displacement calculated by integration of the velocity waveform. (*c*) High-pass-filtered cupular displacement. (*d*) Envelope of cupular displacement (*c*). (*e*) Ratio of the envelope of cupular displacement (*d*) to the envelope of the stimulus. The stimulus envelope remains constant throughout the experiment. It is convenient to choose its maximum value as unity. The corresponding maximum vibrational amplitude of the sphere was 12 μm. The response is linear since the ratio is constant during the modulation cycle, while its magnitude is equal to the maximum of the cupular vibrational amplitude, which in this case was ≈125 nm.

carrier provides a continuous range of amplitudes, enabling the determination of nonlinearity with high resolution.

All (five of the seven investigated in this study) cupulae exhibiting normal frequency tuning (cf. ref. 10) showed similar responses. Results of a cupula with a resonance frequency of 275 Hz are presented in Fig. 3. At a low carrier frequency (126 Hz), the cupular response is linear as evidenced by the flat ratio curve (Fig. 2). At a higher carrier frequency (210 Hz), the ratio is higher in magnitude because of the frequency tuning of the cupula (10), but it also exhibits a broad maximum during the middle of the modulation cycle. The change in the ratio indicates nonlinear behavior of the cupula. This appears to happen when the envelope of the displacement exceeds the range of 100–200 nm. Well above the resonance frequency (410 Hz), the largest changes in ratio occur at the beginning and end of the modulation cycle.

To determine whether the observed nonlinear effects originated in the hair cells, we applied quinine to the lateral-line organ. Recently, it was shown that quinine expels hair cells from the sensory epithelium and mechanically uncouples the cupula from the sensory epithelium (23). Indeed, as shown in Fig. 4, application of 4 mM quinine hydrochloride severely reduces the nonlinear behavior of the cupula.

Comparison with a Model. To investigate to what extent the observed nonlinear responses may be explained by the kinetics of the gating springs, a recently developed model was

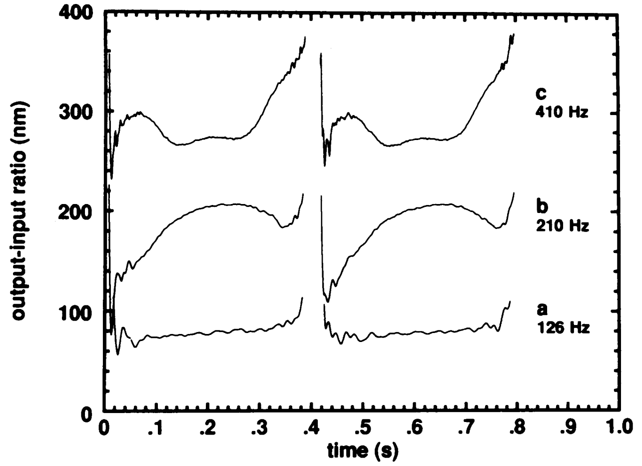

FIG. 3. Output/input ratio of the envelopes of cupular displacement to the envelope of the (normalized) stimulus as a function of time. The carrier frequencies are 126 Hz (*a*), 210 Hz (*b*), and 410 Hz (*c*). At 126 Hz, the ratio of the envelope of the response to the envelope of the stimulus does not change appreciably during the modulation cycle. Therefore, the response is, in good approximation, linear. At 210 Hz, the ratio changes, indicating that the cupular displacement increases nonlinearly with the input. At about 0.2 and 0.6 s, the response is a factor of ≈1.5 higher than that expected for a linear system. This increase indicates a decrease in stiffness, because at 210 Hz cupular displacement is inversely proportional to stiffness. At 410 Hz, the ratio also changes during the modulation cycle, showing nonlinearity. At this carrier frequency, where cupular mechanics is predominantly mass-controlled, the interpretation requires the use of the model described in the paper.

used that combines the nonlinear mechanical properties of the gating springs together with the hydrodynamics and frequency selectivity of the cupula. The equation of motion of the cupula in this model is given by (14):

$$M\frac{d^2X}{dt^2} = M^*\frac{d^2D}{dt^2} + F_{\text{fluid}} - S_{\text{piv.}}X - F_{\text{g.s.}}(X). \qquad [1]$$

In Eq. **1**, X is cupular displacement, D is canal fluid displacement, $F_{\text{g.s.}}$ is the force due to the gating springs, M is the mass of the cupula, and M^* is the mass of fluid displaced by it, while $S_{\text{piv.}}X$ is the (linear) part of the hair bundle restoring

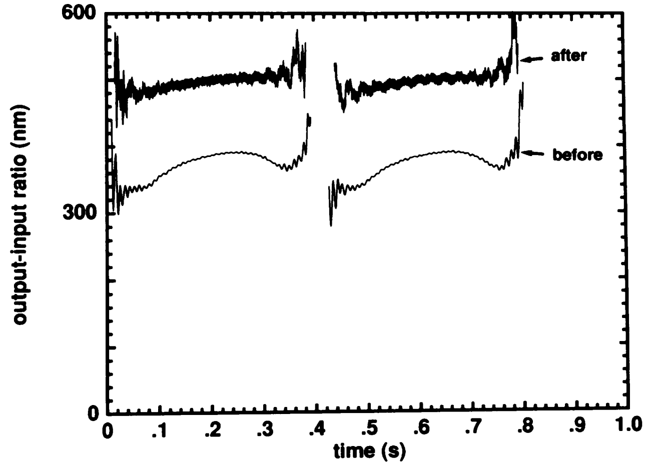

FIG. 4. Output/input ratio of the envelope of cupular displacement to the envelope of the stimulus at 306 Hz as a function of time before and 1.5 hr after administration of 4 mM quinine. The resonance frequency of this cupula was ≈420 Hz. The change in the ratio during the modulation cycle, indicating nonlinear behavior, disappears after the application.

force (24) related to the pivoting stiffness. The force F_{fluid}, exerted on a moving (hemi-)sphere with radius a ($4 \cdot 10^{-4}$ m) by a fluid with viscosity μ (0.015 kg/(m·s), is approximated by

$$-6\pi a\mu\left[\frac{dX}{dt}-\frac{dD}{dt}\right]-\frac{1}{2}M^{*}\left[\frac{d^{2}X}{dt^{2}}-\frac{d^{2}D}{dt^{2}}\right].$$

An expression for $F_{\mathrm{g.s.}}(X)$ can be derived from the model of Howard and Hudspeth (8). When applied to the stiffness of the hair bundles attached to the cupula, the two groups of morphologically polarized hair cells have to be taken into account (14). Assuming N identical gating springs, this yields for $F_{\mathrm{g.s.}}(X)$ and the related stiffness $S_{\mathrm{g.s.}}(X) = dF_{\mathrm{g.s.}}(X)/dX$:

$$F_{\mathrm{g.s.}}(X) = NK_{\mathrm{g.s.}}\gamma\left\{\gamma X-\frac{d}{4}\left[\tanh\frac{K_{\mathrm{g.s.}}\gamma d(X-X_{0})}{2kT}\right] + \frac{d}{4}\left[\tanh\frac{K_{\mathrm{g.s.}}\gamma d(-X-X_{0})}{2kT}\right]\right\} \qquad [2]$$

and

$$S_{\mathrm{g.s.}}(X) = NK_{\mathrm{g.s.}}\gamma^{2}\left\{1-R\left[\cosh\frac{K_{\mathrm{g.s.}}\gamma d(X-X_{0})}{2kT}\right]^{-2} - R\left[\cosh\frac{K_{\mathrm{g.s.}}\gamma d(-X-X_{0})}{2kT}\right]^{-2}\right\}, \qquad [3]$$

where $K_{\mathrm{g.s.}}$ is the spring constant of the gating spring, d is the swing of the gating spring, k is Boltzmann's constant, T is the absolute temperature, $R = K_{\mathrm{g.s.}}d^{2}/8kT$, and X_0 is the deflection of the cupula at which half the transduction channels are open and where γ is a lever ratio of extension of a gating spring to stereociliar deflection (e.g., see ref. 8).

The profiles of (total) force and stiffness used are shown in Fig. 5 and are based on the following parameters. The value of the gating force, $K_{\mathrm{g.s.}}\gamma d$ ($\approx$100 fN), is of the same order of magnitude as the values reported for hair cells *in vitro* [$\approx$300 fN (8); $\approx$100 fN (13)]. The number of gating springs involved (N) is $\approx 1.4 \cdot 10^{6}$. This number, divided by the average value of $\approx$5000 hair cells underlying a cupula, would amount to almost 300 gating springs per hair bundle. This number is of the same order as the number found in saccular hair cells ($\approx$85). X_0 was 123 nm.

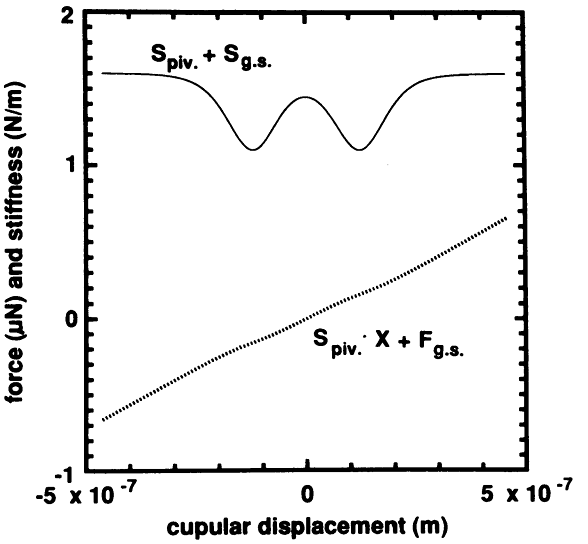

FIG. 5. Stiffness ($S_{\mathrm{piv.}} + S_{\mathrm{g.s.}}$) and force ($S_{\mathrm{piv.}}X + F_{\mathrm{g.s.}}$) exerted by the hair bundles on the cupula as a function of cupular displacement, X, as used to calculate the displacement of the cupula. The stiffness is symmetrical around zero displacement corresponding to the two groups of morphologically polarized hair cell populations underlying the cupula. The nonlinear force due to the gating springs produces the bumps in the curves.

Eq. 1 was solved for X in the time domain by using a fourth-order Runge–Kutta algorithm with the amplitude-modulated fluid displacement used during the experiments, $D(t) = D_0[1 + \sin(2\pi f_m t)]\sin(2\pi f_c t)$, where D_0 is peak fluid displacement, f_m is the modulation frequency (2.4 Hz), and f_c is the carrier frequency (see Fig. 2*a*). Results are shown in Fig. 6 at the same carrier frequencies as shown in Fig. 4.

At 126 Hz the ratio is flat, indicating a linear response, corresponding to that observed in the experiments (Fig. 3*a*). At 210 Hz, the ratio changes during the modulation cycle and shows a maximum. This change is similar to that found experimentally (Fig. 3*b*). At frequencies well above resonance (410 Hz), the model results also agree with the measured responses (Fig. 3*c*).

The ratio curves in both experimental (Fig. 3) and model (Fig. 6) results are asymmetrical with respect to time (0.205 and 0.615 s). This asymmetry can be understood from the group delay ($d\phi/d\omega$) of the cupular displacement, resulting in a slight time delay of the response envelope with respect to the stimulus envelope.

DISCUSSION

Nonlinear cupular dynamics has been observed in the lateral-line organ of living fish by using a noninvasive, optical method. Because the nonlinearity disappears when the cupula is uncoupled from the hair bundles, we conclude that the mechanical properties of the hair cell bundles cause this nonlinear behavior.

Previous analysis has shown that the displacement of the cupula is inversely proportional to its stiffness at frequencies well below the resonance frequency (10, 22). Therefore, changes in hair bundle stiffness can most easily be interpreted at frequencies in this "stiffness-controlled" range. The measured increase of the output/input ratio during the time intervals that the input amplitude increases (cf. Fig. 3*b*) indicates that the stereociliar stiffness decreases with increasing vibrational amplitude.

A quantitative interpretation of the measurements on the fluid–cupula–hair cell complex requires an analysis that prop-

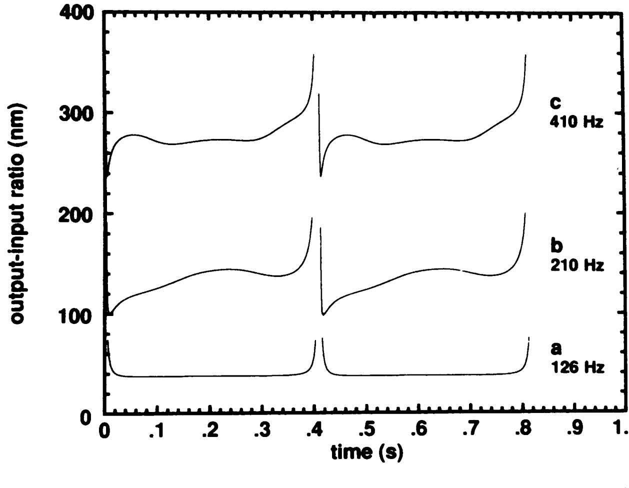

FIG. 6. Ratio of the envelopes of cupular responses to the envelope of the stimulus as a function of time, as predicted by the model. The ratio curves were calculated at the same carrier frequencies as used for the experimental results (126, 210, and 410 Hz) and show similar nonlinear behavior (cf. Fig. 3).

erly accounts for frequency selectivity of the cupula in combination with nonlinear properties of the hair bundles. Therefore, to test whether the observed nonlinearity can be attributed to the nonlinear stiffness of the gating springs, we used a nonlinear, hydrodynamic model of the cupula. The model predicts that the mechanical characteristics of the nonlinear gating springs are most clearly reflected in the cupular responses at (carrier) frequencies below and above the resonance frequency. At these frequencies, the model results mimic closely the results obtained from the measurements.

We therefore conclude that the observed nonlinearity in cupular mechanics *in vivo* may be due to the gating compliance resulting from the opening and closing of the transduction channels.

We thank Dr. Alfons B. A. Kroese and Profs. H. Duifhuis and D. G. Stavenga for critically reading the manuscript and for helpful suggestions for improvement. This research was supported by Program Project Grant DC00316 from National Institute on Deafness and Other Communication Disorders, by the Emil Capita Foundation, and by a Fellowship of the Royal Netherlands Academy of Arts and Sciences to S.M.v.N.

1. Howard, J., Roberts, W. M. & Hudspeth, A. J. (1988) *Annu. Rev. Biophys. Biophys. Chem.* **17**, 99–124.
2. Hudspeth, A. J. (1989) *Nature (London)* **341**, 397–404.
3. Pickles, J. O. & Corey, D. P. (1992) *Trends Neurosci.* **15**, 254–259.
4. Hudspeth, A. J. (1983) *Annu. Rev. Neurosci.* **6**, 187–215.
5. Jaramillo, F. & Hudspeth, A. J. (1991) *Neuron* **7**, 409–420.
6. Pickles, J. O., Comis, S. D. & Osborne, M. P. (1984) *Hearing Res.* **15**, 103–112.
7. Corey, D. P. & Hudspeth, A. J. (1983) *J. Neurosci.* **3**, 962–976.
8. Howard, J. & Hudspeth, A. J. (1988) *Neuron* **1**, 189–199.
9. Russell, I. J., Kössl, M. & Richardson, G. P. (1992) *Proc. R. Soc. London. B* **250**, 217–227.
10. van Netten, S. M. & Kroese, A. B. A. (1987) *Hearing Res.* **29**, 55–61.
11. van Netten, S. M., Kelly, J. P. & Khanna, S. M. (1990) in *Abstracts of the 13th Midwinter Research Meeting 1990* (Association for Research in Otolaryngology, St. Petersburg Beach, FL), pp. 341–342 (abstr.).
12. van Netten, S. M. & Kroese, A. B. A. (1989) in *Cochlear Mechanisms: Structure, Function and Models*, eds. Wilson, J. P. & Kemp, D. T. (Plenum, New York), pp. 47–55.
13. Jaramillo, F. & Hudspeth, A. J. (1993) *Proc. Natl. Acad. Sci. USA* **90**, 1330–1334.
14. van Netten, S. M. (1993) in *Biophysics of Hair Cell Sensory Systems*, eds. Duifhuis, H., Horst, J. W., van Dijk, P. & van Netten, S. M. (World Scientific, Singapore), pp. 391–397.
15. Oswald, R. L. (1978) *Comp. Biochem. Physiol.* **60**, 19–26.
16. Khanna, S. M., Rosskothen, H. & Koester, C. J. (1989) *Acta Oto-Laryngol. Suppl.* **467**, 51–59.
17. Koester, C. J. (1980) *Appl. Opt.* **19**, 1749–1757.
18. Koester, C. J., Khanna, S. M., Rosskothen, H. & Tackaberry, R. B. (1989) *Acta Oto-Laryngol. Suppl.* **467**, 27–33.
19. Willemin, J. F., Dändliker, R. & Khanna, S. M. (1988) *J. Acoust. Soc. Am.* **83**, 787–795.
20. Willemin, J. F., Khanna, S. M. & Dändliker, R. (1989) *Acta Oto-Laryngol. Suppl.* **467**, 35–42.
21. Kelly, J. P. & van Netten, S. M. (1991) *J. Morphol.* **207**, 23–36.
22. van Netten, S. M. (1991) *J. Acoust. Soc. Am.* **89**, 310–319.
23. van Netten, S. M., Karlsson, K. K., Khanna, S. M. & Flock, Å. (1994) *Hearing Res.*, in press.
24. Crawford, A. C. & Fettiplace, R. (1985) *J. Physiol.* **364**, 359–379.